Published in final edited form as:
Clin Cancer Res. 2013 November 1; 19(21): . doi:10.1158/1078-0432.CCR-13-0850.

Dual blockade of the PI3K/AKT/mTOR (AZD8055) and RAS/MEK/ERK (AZD6244) pathways synergistically inhibits rhabdomyosarcoma cell growth *in vitro* and *in vivo*

Jane Renshaw[1,2], **Kathryn R. Taylor**[1,2], **Ryan Bishop**[1,2], **Melanie Valenti**[2], **Alexis De Haven Brandon**[2], **Sharon Gowan**[2], **Suzanne A. Eccles**[2], **Ruth R. Ruddle**[2], **Louise D. Johnson**[2], **Florence I. Raynaud**[2], **Joanna L. Selfe**[2,3], **Khin Thway**[2,3,4], **Torsten Pietsch**[5], **Andrew D. Pearson**[1], and **Janet Shipley**[2,3]

[1]Division of Clinical Studies, The Institute of Cancer Research, Sutton, Surrey. UK

[2]Division of Cancer Therapeutics, The Institute of Cancer Research, Sutton, Surrey. UK

[3]Division of Molecular Pathology, The Institute of Cancer Research, Sutton, Surrey. UK

[4]Histopathology Department, The Royal Marsden Hospital NHS Foundation Trust, London, UK

[5]Department of Neuropathology, University of Bonn, D-53105, Germany

Abstract

Purpose—To provide rationale for using PI3K and/or MAPK pathway inhibitors to treat rhabdomyosarcomas (RMS), a major cause of pediatric/adolescent cancer deaths.

Experimental design—The prevalence of PI3K/MAPK pathway activation in RMS clinical samples was assessed using immunohistochemistry. Compensatory signaling and crosstalk between PI3K/MAPK pathways was determined in RMS cell lines following p110α shRNA-mediated depletion. Pharmacological inhibition of reprogrammed signaling in stable p110α knockdown lines was used to determine the target-inhibition profile inducing maximal growth inhibition. The *in vitro* and *in vivo* efficacy of inhibitors of TORC1/2(AZD8055), MEK(AZD6244) and P13K/mTOR(NVP-BEZ235) were evaluated alone and in pair-wise combinations.

Results—PI3K pathway activation was seen in 82.5% rhabdomyosarcomas with co-activated MAPK in 36% and 46% of alveolar and embryonal sub-types respectively. p110α knockdown in cell lines over the short and long term was associated with compensatory expression of other p110 isoforms, activation of the MAPK pathway and cross-talk to reactivate the PI3K pathway. Combinations of PI3K pathway and MEK inhibitors synergistically inhibited cell growth *in vitro*. Treatment of RD cells with AZD8055 plus AZD6244 blocked reciprocal pathway activation, as evidenced by reduced AKT/ERK/S6 phosphorylation. *In vivo*, the synergistic effect on growth and changes in pharmacodynamic biomarkers was recapitulated using the AZD8055/AZD6244 combination but not NVP-BEZ235/AZD6244. Pharmacokinetic analysis provided evidence of drug-drug interaction with both combinations.

Corresponding authors: Jane Renshaw and Janet Shipley, Sarcoma Molecular Pathology Team, Divisions of Molecular Pathology and Cancer Therapeutics, The Institute of Cancer Research, 15 Cotswold Road, Sutton Surrey SM2 5NG, UK Tel: 00 44 20 8722 4327 and 4273 jane.renshaw@icr.ac.uk, janet.shipley@icr.ac.uk.

Disclosure of Potential Conflicts of Interest: JR, MV, ADHB, SG, SAE, RRR, LDJ, FIR, JLS, ADP and JS are current employees of The Institute of Cancer Research, which has a commercial interest in the development of PI3K pathway inhibitors and operates a rewards for inventors scheme.

Europe PMC Funders Author Manuscripts

Conclusions—Dual PI3K/MAPK pathway activation and compensatory signaling in both rhabdomyosarcoma subtypes predicts a lack of clinical efficacy for single agents targeting either pathway, supporting a therapeutic strategy combining a TORC1/2 with a MEK inhibitor.

Keywords

Rhabdomyosarcoma; PI3K pathway inhibitors; MAPK pathway inhibitor; synergistic inhibition; pharmacodynamics/pharmacokinetics

Introduction

Rhabdomyosarcomas (RMS) are the most common soft tissue sarcomas in children aged 0-14 years, accounting for around 50% of all cases in this age group (Reviewed in (1)). The two major histological subtypes, Alveolar (ARMS) and Embryonal (ERMS) carry distinct morphological and genetic alterations: The majority of ARMS harbor PAX3-FOXO1 or PAX7-FOXO1 chimeric transcription factors (2), and the presence of the *PAX3-FOXO1* fusion transcript has been associated with poor prognosis (3). ERMS generally have a more favorable outcome and carry no consistent chromosomal translocations, although allelic imbalances at 11p15.5 are commonly identified (1, 2). Dysregulation of the RAS signaling pathway is likely relevant to the pathogenesis of ERMS (4, 5), and also IGF signaling to the pathogenesis of all RMS (6). The use of multi-agent chemotherapy, surgery and radiation has improved the outcome for RMS patients with favorable features, although at a cost of disfigurement and long term sequelae (7). Unfortunately, the prognosis for metastatic and relapsed RMS tumors remains poor and the need for novel, less toxic therapeutic strategies is pressing.

High levels of phosphorylated AKT have been reported in RMS cell lines and a significant proportion of primary tumors indicative of constitutive activation of the PI3K/AKT/mTOR pathway, and suggesting that RMS may be sensitive to the targeted inhibition of this pathway (8, 9). However, previous reports in other tumor types have indicated that activated MAPK signaling mediates resistance to PI3K inhibitors (10, 11). Indeed, *NRAS* mutations, identified in approximately 20% of ERMS patients (4), may identify those tumors unlikely to respond to PI3K inhibitors, as has been shown for KRAS mutated lung cancers (10). Conversely, intrinsic resistance to MEK inhibitors has been associated with strong PI3K signaling in colorectal and breast cancer cell lines (12, 13). Thus dual activation of both PI3K/AKT/mTOR and RAS/RAF/MEK/ERK pathways is likely to result in resistance to the targeting of either pathway alone. Encouragingly, co-inhibition of both pathways has shown utility in reducing tumor growth in a variety of xenograft cancer models (10, 13-15), and clinical trials of such combinations are underway in adults.

Here we assessed the prevalence of co-activation of the PI3K and MAPK pathways in a large series of well-characterized RMS clinical samples by performing immunohistochemistry for phosphorylated markers of both pathways, as well as downstream S6. We used shRNA-induced p110α knockdown (KD) to explore compensatory signaling and crosstalk between the PI3K/MAPK pathways in RMS cell lines and performed comprehensive preclinical *in vitro* and *in vivo* studies of PI3K and/or MAPK pathway targeted therapies. We provide evidence to support the class of PI3K inhibitor that is most effective, identify mechanisms likely to be responsible for treatment failure and undertook combination studies that address this problem. Our results predict a general lack of clinical efficacy of PI3K/AKT/mTOR or RAS/RAF/ERK pathway monotherapy in RMS and we propose a dual targeted strategy for clinical testing.

Europe PMC Funders Author Manuscripts

Materials and Methods

RMS tissue from patients and immunohistochemistry

A tissue microarray (TMA) of formalin-fixed, paraffin-embedded diagnostic tumor material from 79 patients with RMS (25 alveolar and 54 embryonal by histology) with approval for the study, (Local Research Ethics Committee protocol Nos 1836 and 2015 and Multi-Regional Research Ethics Committee/06/4/71), has been described previously (16). Following antigen retrieval (0.1M sodium citrate, pH 6.0, microwave 600W, 30mins), and blocking (TBS with 5% milk, 2% normal rabbit serum, 30mins), TMA sections (4μm) were immunostained using antibodies against phospho-AKT(Ser473), phosphor-ERK1/2(Thr202/Tyr204) and phospho-S6(Ser235/236),(1:200 dilution, Cell Signaling Technology) with detection using the avidin-biotin complex method (DAKO) visualized by diaminobenzidine tetrahydrochloride (DAB). Slides were lightly counterstained with hematoxylin. Cores were scored blind by a pathologist as negative, weak, moderate or strong for intensity and were considered to be positive if at least 10% of cells in the core showed staining.

Cell culture, compounds and GI_{50} estimation

The source of the human tumor cell lines RH30, RMS-1, SCMC, and RH41 derived from ARMS, and RD, RMS-YM and CT10 derived from ERMS is described elsewhere (16). All cell lines were grown in DMEM (Sigma UK) supplemented with 10% fetal bovine serum (Biosera, Labtech International Ltd,) in 5% CO_2 in air at 37°C. Cell line identity was validated by analyzing short tandem repeats using the Promega Power Plex 1.2 system, according to the manufacturers' instructions, within six months of the experiments described. Results were matched with those available from repositories which hold the lines (RH30 and RD) or those produced immediately after delivery of the cell lines to our laboratory. All compounds were purchased from AxonMed Chem, except NVP-BMK120 (Selleckchem). Compounds were dissolved in the appropriate solvent at 10mM and diluted in tissue culture medium to working concentrations. GI_{50} values, (concentrations causing 50% inhibition of cell proliferation after 72hr continuous exposure), were determined in 96 well plates using the MTS assay (Promega). For the construction of isobolograms, the GI_{50} values of compound A and B were determined along with the GI_{50} values of compound B in the presence of various fixed sub GI_{50} concentrations of compound A. The GI_{50} values of compound A and B were then plotted on the x and y axes along with the GI_{50} values of compound B versus the fixed concentration of compound A.

Lentiviral shRNA KD of *PIK3CA*, Western Blotting and FACS analysis

Lentiviral particles for shRNA KD of *PIK3CA* were produced following transfection of the lentiviral packaging vectors pMD2.G (3μg), pMDLg/RRE (5μg) and pRSV-Rev (2.5μg, Addgene), and either the *PIK3CA* shRNA vector (10μg, TRCN0000039603, Sigma) or the control shRNA vector (10μg, SHCOO2, Sigma) into HEK293T cells as described previously (16). Control (CONSH) or *PIK3CA* shRNA LV particles were transduced into RH30, RMS-1, RD and RMS-YM cells (in 2× 6 well plates per line) at a multiplicity of infection of 10 in the presence of polybrene (4μg/ml, Sigma Aldrich) and transduced cells were selected with puromycin (2.5μg/ml) from day 2. On days 2, 5 and 8 viable cells were counted (ViCell series automated Cell Viability Analyzer, Beckman Coulter), cells fixed with 70% ethanol for fluorescence-activated cell sorting (FACS) analysis, and proteins extracted for Western Blotting.

For Western blotting, following quantitation (BCA Protein Assay Kit (Pierce), 10μg each lysate were separated using NuPage Bis-Tris or Tris-Acetate gels (Invitrogen), transferred onto Highbond PVDF membranes (Amersham Biosciences) and probed with 1:1,000 dilution of primary antibody (Cell Signaling Technology) overnight at 4°C, and 1:10,000

dilution of horseradish peroxidase secondary antibody (Amersham Biosciences) for 2h at room temperature. Signal was detected with ECL Plus reagent (Amersham) and visualized and analyzed using a STORM 860 PhosphorImager and ImageQuant® software (AmershamBiosciences).

For FACS analysis, fixed cells were spun, resuspended in 800μl PBS, 100μl RNase (0.1mg) and 100μl PI (propidium iodide, 40μg) and incubated at 37°C for 30 minutes. Labeled cells were stored at 4°C until cell cycle analysis on a BDLSRII FACS analyzer (BD Franklin Lakes, NJ USA) using BDFACSDiVa software with doublet discrimination. For each sample 10,000 events were recorded.

Pharmacodynamic (PD), Pharmacokinetic (PK) and Xenograft Efficacy studies

All animal experiments were conducted in accordance with United Kingdom Home Office Regulations under the Animals (Scientific Procedures) Act 1986 and United Kingdom Co-coordinating Committee on Cancer Research guidelines (17). RD cells (5×10^6 cells in 25% matrigel, BD Biosciences) were subcutaneously implanted bilaterally (for initial PD and PK studies), or in one flank (for tumor efficacy studies) into female 6-8 week old CrTac:Ncr-*Fox1(nu)* (Ncr) athymic mice (Charles River). AZD6244, (10mg/kg in 10%DMSO water), AZD8055, (10 or 20mg/kg in acidified water) and NVP-BEZ235 (25mg/kg in 10% NMP in 90% PEG300) were given orally (0.1mL/10g body weight of vehicle) alone, or in combination. Control animals received the equivalent volume of appropriate vehicle(s). For initial PK and PD analysis, mice (n=3) bearing tumors of sufficient size were euthanized at various times following dosing, tumors were excised, bisected and snap frozen, and blood was collected, centrifuged and the plasma frozen for storage at −80°C. For tumor efficacy studies, dosing commenced when the tumors were well established (≈5 mm mean diameter, n=6/treatment group) and continued daily for 19-22 days. Animals were weighed at regular intervals and observed for adverse effects. Tumors were measured across two perpendicular diameters, and volumes were calculated using the formula $V=4/3\pi[(d1+d2)/4]^3$. On termination of the experiment, mice were bled, tumors were excised and weighed, and samples processed as described above.

Quantitative PK analysis was done by liquid chromatography tandem mass spectrometry and multiple reaction monitoring, using a modification of the previously described method ((18) and Suppl methods). Tumor PD biomarkers were assessed by a Meso Scale Discovery multispot electrochemiluminescence immunoassay system to detect phospho(T/Y: 202/204:185/187)ERK/total ERK1/2, phospho(Ser473)AKT/total AKT and phospho(240/244)S6/total S6 in 10μg tumor lysate according to manufacturers' instructions.

Results

Dual activation of the PI3K and MAPK pathways is prevalent in primary rhabdomyosarcomas

36% (8/22) ARMS and 46% (19/41) ERMS samples stained positively for both p-AKT and p-ERK. Of these, 50% (4/8) ARMS and 58% (11/19) ERMS samples also stained positively for p-S6 indicating strong activation of mTOR signaling. 59% (13/22) of ARMS but only 29% (12/41) ERMS samples stained positively for p-AKT but not p-ERK suggesting that ERMS patients may be less likely than ARMS patients to respond to single agent PI3K pathway inhibition. Notably, 93% (27/29) samples staining positively for pERK also stained positively for pAKT which, in addition to samples with no detectable pERK staining and high levels of pAKT could predict resistance to MAPK pathway inhibitors in the majority of RMS. Assessment of correlation between staining using chi squared tests for trend showed a significantly positive correlation in all pairwise analyses: pAKT and pERK trend statistic:

4.0912 (p=0.0431), pAKT and pS6 trend statistic: 8.5413 (p=0.0035), pERK and pS6 trend statistic: 11.1429 (p=0.0008) (Suppl Tables S1A-C).

PIK3CA KD induces widespread compensatory signaling and reciprocal cross-talk between the MAPK and PI3K pathways

Consistent with previous reports that the PI3K p110α and β isoforms are expressed ubiquitously (reviewed in (19)), p110α was found to be expressed at similar levels in a panel of seven RMS cell lines, while p110β expression was more variable (Supp Fig S1). Unexpectedly p110δ, expressed predominantly in leukocytes (19), was expressed at high level in two (RH30 and RH41) of the four ARMS but none of the ERMS lines studied here. PI3K p110α, (encoded by *PIK3CA*), has been suggested to be the isoform that is predominantly involved in insulin, IGF signaling and cell growth in many cell types (reviewed in (19)). To assess the importance of PI3K p110α to the growth and survival of RMS cell lines, two ARMS lines (RH30 and RMS-1), and two ERMS lines (RD and RMS-YM) were transduced with lentiviral (LV) shRNA particles targeted to *PIK3CA*. None of these lines carry an oncogenic *PIK3CA* mutation. Only the ARMS line, RMS-1, was growth inhibited in response p110α KD (Fig 1A). Growth inhibition did not involve cell cycle arrest as evidenced by FACS analysis (Suppl Fig S2), nor did there appear to be increased apoptosis (PARP cleavage) or autophagy (LC3BII production) (Fig 1B) indicating cytostasis.

KD of p110α induced varying degrees of compensatory upregulation of p110β expression in all four cell lines (Fig 1B), while p110δ expression was minimally affected. Downstream, AKT phosphorylation was not consistently inhibited following KD of p110α (Figure 1C). Of note, increased $p^{Thr\ 308}$Akt to above control levels, (not mirrored by an equivalent increase in p^{Ser473}Akt), was seen on day 5 following LV transduction of RH30 cells, with gross inhibition of AKT phosphorylation being delayed until day 8. By contrast, both $p^{Thr\ 308}$Akt and p^{Ser473}Akt were reduced to below control levels in RMS-1, RD and RMS-YM cells by day 5 with recovery towards control levels in the ERMS lines by day 8. In addition, PTEN expression was downregulated in RH30 cells but increased in the remaining three cell lines (quantitation shown in Suppl Fig S3). Inhibition of downstream S6 phosphorylation mirrored inhibition of AKT phosphorylation in all cell lines except RH30, where inhibition of S6 and AKT phosphorylation appeared disconnected. The latter may reflect signaling from p110α through only one of the three AKT isoforms to mTOR, leading to decreased S6 phosphorylation despite an apparent lack of inhibition of total AKT phosphorylation.

Classical relief of IRS2 (but not IRS1, data not shown), feedback repression on inhibition of mTOR signaling (20) was seen in three of the cell lines (exception, RH30), as well as evidence of reciprocal cross-talk between the PI3K/AKT/mTOR and RAS/RAF/ERK pathways. Varying degrees of up-regulation of pERK1/2 by day 5 following LV transduction were observed in the three p110α KD resistant cell lines, but not until day 8 in the sensitive RMS-1 cells. Evidence of transient activation of AMPK concomitant with up-regulated pERK (21) was observed in three cell lines, (exception RD, where pAMPK levels were reduced). Quantitation of the pERK1/2 and total ERK1/2 Western blots confirmed both a higher basal activation of ERK signaling in the ERMS compared to the ARMS lines and the stimulation of ERK phosphorylation following *PIK3CA* KD (Fig 1D).

Pharmacological inhibition of re-programmed signaling pathways in *PIK3CA* KD stable cell lines establishes the rationale for dual blockade of the PI3K/MAPK pathways in RMS

To determine the long-term effects of reduced *PIK3CA* expression on PI3K and MAPK signaling, stable p110α KD and control (CONSH) cell lines were derived from the virally

transduced cell lines over a period of around 4 weeks. The derived cell lines were then used to screen PI3K pathway inhibitors with a variety of inhibition profiles against the Class 1 p110 isoforms and/or mTOR.

Both ERMS stable KD lines showed increased expression of p110δ, a novel observation consistent with p110δ being downstream of growth factor signaling (19), and functional redundancy between the p110α and δ isoforms (22). No differences in sensitivity to the pan-PI3K inhibitor BMK120, (modestly selective for p110α versus the other isoforms (Suppl Fig S4A)) was observed in the stable p110α KD lines and their CONSH counterparts (Suppl Fig S4B). In addition, only the RMS-1 stable KD cell line, with minimal p110α and δ expression, showed increased sensitivity to the p110β inhibitor, TGX221 (78-fold selective for p110β versus p110α, less so for p110δ, Suppl Fig S4A and C). Taken together, these data show that all expressed isoforms must be inhibited for maximum inhibition of cell growth.

Assessment of selected elements of the PI3K/AKT/mTOR and RAS/RAF/ERK pathways in the stable KD lines (Fig 2A) revealed increased p^{Thr308}AKT but not p^{Ser473}AKT levels in three of the four stable KD lines (exception, RMS-YM), which was accompanied by altered PTEN expression in the RD stable KD line. Increased levels of p^{Thr308}AKT correlated with increased phosphorylation of GSK3β, a downstream AKT substrate, but did not have a consistent impact on pS6 levels (Suppl Fig S4D). IRS2 expression was upregulated in the RMS-1, RD and RMS-YM stable KD lines suggesting that increased signaling through IGF1R may contribute to increased p^{Thr308}AKT in some cell lines. Upregulated MAPK signaling, as evidenced by increased pERK levels, was observed in all the stable KD lines resulting in crosstalk that substantially increased pAMPK levels and, in the ERMS KD lines, increased the basal rate of autophagy (LCB3II production). These latter data are consistent with disruption of aspects of mTOR signaling in these cell lines. Treatment with NVP-BEZ235, which predominantly inhibits mTOR at concentrations of less than 100nM (23), and AZD8055, a specific TORC1/2 inhibitor, demonstrated that the p110α stable KD cell lines with deregulated IRS2 expression are more sensitive to mTOR inhibition than their CONSH counterparts (Figs 2B and C). In addition, stable KD lines exhibited increased sensitivity to ZSTK474, a pan PI3K inhibitor with selectivity for p110δ, and modest activity against mTor (IC_{50} of 0.377μM (24)),(Suppl Figs S4A and E). Although all the stable KD lines expressed increased pERK levels, only the RMS-1 KD line (lacking both p110α and p110δ) exhibited significantly enhanced sensitivity to the MEK inhibitor AZD6244 (Fig 2D). This suggests that p110α and/or p110δ can support compensatory signaling through PI3K/AKT/mTOR on inhibition of the MAPK pathway, whereas p110β cannot.

Overall, these data suggest that not only should pan-PI3K (or AKT) and mTOR activity be inhibited in order to achieve maximal inhibition of the PI3K/AKT/mTOR pathway, but simultaneous inhibition of the RAS/RAF/ERK pathway to prevent compensatory cross talk is necessary to maximize the anti-proliferative effect.

Dual blockade of PI3K/AKT/mTOR and RAS/RAF/ERK signaling is synergistic in RMS cell lines

To determine whether dual blockade of both the PI3K and MAPK pathways yields improved efficacy in RMS cells, combination GI_{50} isobolograms were constructed using the parental ARMS and ERMS cell lines and the combinations AZD8055/AZD6244, ZSTK474/AZD6244 and NVP-BEZ235/AZD6244. The combination AZD8055/AZD6244 was synergistic in the RH30, RD and RMS-YM cell lines, but nearer additive in the RMS-1 line (the most sensitive line to single-agent PI3K pathway inhibition) (Fig 3A). The ERMS cell lines were used to confirm synergy with the combinations ZSTK474/AZD6244 and NVP-BEZ235/AZD6244 (Figs 3B and C).

RD cells that have an *NRAS* mutation (5) and are relatively resistant to both AZD8055 and AZD6244, were selected to investigate the effect of single-agent and combination treatment with AZD8055 and AZD6244 on the biomarkers of PI3K/mTOR pathway (p^{Ser473}AKT and pS6) and MAPK pathway (pERK) activity over a 48hr time course. To more easily assess any synergistic effects on the pathway biomarkers following combination treatment, cells were treated with 0.5×, and 1.0× GI_{50} concentrations. AZD8055 increased pERK levels, and AZD6244 increased p^{Ser473}AKT levels after 16hrs treatment, confirming reciprocal compensatory cross-talk between the PI3K and MAPK pathways following inhibition of each pathway individually (Fig 3D). The extent of inhibition of S6, but not AKT phosphorylation, was concentration dependent following AZD8055 treatment indicating that at low concentrations, and with activating cross-talk from the MAPK pathway, TORC1 was more effectively inhibited than TORC2. AZD6244 treatment ablated pERK levels at all time points and both concentrations and the activation/inhibition profiles of both AKT and S6 phosphorylation respectively, were similar at both concentrations. These data indicate that growth inhibition following AZD6244 does not correlate with MEK inhibition, (IC_{50} concentration for MEK1/2 of 14nM (25)), and may be due to off target effects.

AZD6244 in combination with AZD8055 reduced pERK levels to the same extent as AZD6244 alone, while pS6 levels were reduced earlier, to a greater extent, and for a longer duration than with either treatment alone (Fig 3D). AKT phosphorylation was reduced to the same extent as treatment with AZD8055 alone but did not recover to control levels at later time points. These data imply that significant and protracted inhibition of mTOR activity is essential for maximal antitumor activity and that co-inhibition of ERK and AKT signaling is necessary to achieve this.

Equivalent alterations to biomarkers of the PI3K and MAPK pathways occurred *in vivo* 6 hours following treatment of mice bearing RD xenografts with AZD8055 (10mg/kg p.o) and AZD6244 (10mg/kg p.o.) alone, or in combination (Suppl Fig S5A). However, levels of all three biomarkers recovered to control levels or above by 16hrs following treatment and correlated with plasma clearance of both drugs to close to, or below, the limit of detection at this time point (Suppl Fig S5B). This and further PK analysis (Suppl Fig S6) revealed an interaction between both drugs when given in combination. Peak plasma concentrations of AZD6244 were reduced and the elimination phase extended when given in combination with AZD8055, whereas higher plasma and tumor levels of AZD8055 were achieved when given in combination AZD6244. These changes became more pronounced on repeat dosing. The possibility of interaction at the level of metabolism by P450 enzymes was eliminated using a drug-drug interaction assay (Suppl. Methods, data not shown).

Significantly enhanced antitumor efficacy following treatment of RD xenograft tumors with AZD8055, but not NVP-BEZ235, in combination with AZD6244

A preliminary dose-finding therapeutic study defined a once daily treatment schedule of AZD8055, 20mg/kg p.o., and AZD6244, 10mg/kg p.o., as well tolerated and active when given in combination (Suppl Fig S7A-D). Previous studies have shown that NVP-BEZ235 treatment of Her2-overexpressing breast cancer cells resulted in compensatory activation of ERK signaling, and that the combination of NVP-BEZ235 (25mg/kg) and AZD6244 (8mg/kg) was synergistic *in vivo* (26). NVP-BEZ235 is a dual PI3K/mTORC1/2 inhibitor at the concentrations (above 500nM) likely to be achieved *in vivo* (23), and had the potential to inhibit the compensatory increase in pAKT levels on MEK inhibition more effectively than the specific TORC1/2 inhibitor, AZD8055. Therefore, these two combinations were compared in a head-to-head therapeutic study.

When given alone, NVP-BEZ235 inhibited tumor growth to a greater extent than AZD8055. However, synergism was demonstrated only when using AZD6244 in combination with

AZD8055 and not when used in combination with NVP-BEZ235 (Figs 4A and B). PK analysis of all three drugs demonstrated that when given in combination, NVP-BEZ235 reduced plasma concentrations of AZD6244 to a similar extent as AZD8055 (Fig 4C). The plasma concentrations of AZD8055 and NVP-BEZ235 were in the same range when administered alone, and the concentration range of both drugs was increased when given in combination with AZD6244 (Fig 4C).

Assessment of the PD biomarkers, pERK, pAKT^{Ser473}, and pS6 in treated tumors confirmed reciprocal compensatory signaling on inhibition of either the PI3K pathway by AZD8055 or NVP-BEZ235, or the MAPK pathway by AZD6244 in the *in vivo* therapeutic setting (Fig 4D). Individually, AZD8055 and NVP-BEZ235 were equally efficient in reducing AKT and S6 phosphorylation although AZD8055 increased pERK levels to a greater extent than NVP-BEZ235. However, while treatment with the combination AZD8055 /AZD6244 reduced all three biomarkers to less than 30% control levels, the combination NVP-BEZ235/ AZD6244 failed to reduce pAKT below control levels and there was a corresponding reduction in the inhibition of S6 phosphorylation. Thus the inhibitory potency of NVP-BEZ235 against PI3K and TORC2 was insufficient to block the compensatory upregulation of AKT phosphorylation induced by MEK inhibition in this tumor type *in vivo*. AZD8055/ AZD6244 is therefore the combination indicated to take forward to the clinic.

Discussion

Previous reports have indicated that dual activation of the PI3K/AKT/mTOR and Ras/Raf/ MEK/ERK pathways is likely to result in innate resistance to the targeting of either pathway alone (10-13). While activation of both pathways, individually, has been documented in RMS (4, 5, 8, 9), dual activation status has not been assessed. Using immunohistochemical analysis of TMAs, we have shown dual activation in 43% of primary RMS samples and of these, 55% showed strong activation of mTOR signaling. A higher proportion of ARMS than ERMS samples stained positively for pAKT in the absence of pERK staining (59% and 29% respectively). Thus while theoretically, some ARMS patients might benefit from targeted inhibition of the PI3K pathway, it is less likely to be the case for ERMS patients. Importantly, we provide evidence for compensatory upregulation of the MAPK pathway following PI3K pathway inhibition in RMS, as has been shown in other tumor types (15). This has the potential to circumvent the antiproliferative effect of PI3K pathway inhibitors and result in treatment failure.

Small molecule inhibitors of PI3K mainly target the Class 1 PI3Ks namely p110α, β, δ, and γ, of which only p110α is mutated in cancer (19). PI3K p110α is also the isoform that is predominantly involved in IGF1R signalling, (commonly activated in RMS (6)), and cell growth. Using LV shRNA particles targeted to *PIK3CA*, we demonstrated that only one of four RMS cell lines was growth-inhibited following PI3K p110α KD suggesting that a p110α-specific inhibitor would not have general utility in the RMS clinic. Examination of basal Class 1 PI3K isoform expression profiles in RMS cell lines revealed uniform expression of p110α, more variable expression of p110β and no detectable expression of p110γ. Unexpectedly, previously unreported expression of p110δ, generally restricted to cells of hematopoietic origin, was also seen in two of four ARMS lines. Consistent with this, mining of gene expression profiling data of RMS primary tumor samples (3) revealed higher levels of *PI3KCD* mRNA compared to skeletal muscle (data not shown). High level p110δ expression has also been reported in breast cancer and neuroblastoma cells (27, 28). However in RMS cell lines, neither the expression of p110δ, nor the overall isoform expression profiles was associated with sensitivity/resistance to p110α KD.

Compensatory upregulation and reprogramming of alternative signaling pathways in the short and long term offers clues to the mechanisms of innate and acquired resistance to targeted inhibitors. Here we have shown that cell line-specific, widespread compensatory and adaptive signaling occurs following *PIK3CA* KD, even in the absence of any overt phenotypic effect. Using various PI3K pathway inhibitors and a MEK inhibitor to inhibit these bypass mechanisms in stable p110α KD lines, we have determined which elements of the PI3K and MAPK pathways must be inhibited to achieve a maximum antiproliferative effect.

In the short term, p110α KD induced compensatory upregulation of p110β although this was not maintained in the p110α KD stable lines. However, significant upregulation of p110δ was seen in the ERMS stable KD lines which both highlights the plasticity of PI3K isoform expression and supports functional redundancy, particularly between the p110α and δ isoforms. No difference in the sensitivity to the pan-PI3K inhibitor, BMK120, was seen in the stable p110α KD lines compared to their CONSH counterparts and only the RMS-1 KD line, with minimal p110α and δ expression, showed increased sensitivity to the selective p110β inhibitor, TGX221. These data suggest that pan-PI3K inhibitors should possess potent activity against all Class 1A isoforms to ensure maximum growth-inhibition in RMS.

AKT phosphorylation was not consistently inhibited following p110α KD despite early inhibition of S6 phosphorylation in all four cell lines. Of note, we demonstrated increased p^{Thr308}AKT, delayed gross inhibition of pAKT, and down-regulation of the phosphatase, PTEN, in RH30 cells following *PIK3CA* KD, a novel observation. By contrast, early inhibition of AKT phosphorylation and upregulation of PTEN expression was seen in the other 3 lines. Transcriptional regulation of PTEN has been shown previously in various settings but the functional roles and mechanisms responsible remain poorly understood. For example, decreased PTEN expression on inhibition of mTOR has been reported in cells with loss or inactivation of TSC2 (29) while up-regulation of PTEN in response to activation of *c-Jun*-NH_2 Terminal Kinase, (JNK) (30), and repression of PTEN expression by activated NFκB signalling (31) have also been reported.

Compensatory upregulation of pERK levels following *PIK3CA* KD was observed by day 5 in the three cell lines resistant to the effects of p100α KD but this was delayed in the sensitive RMS-1cells. However, increased levels of ERK phosphorylation were seen in all four stable KD lines. A lack of early stimulation of ERK signaling, together with extremely low levels of basal mTOR activity, may underpin the initial sensitivity of RMS-1 cells to *PIK3CA* KD, while the subsequent upregulation of ERK signaling may have contributed to their ultimate recovery and survival. Although previous reports have suggested that activated MAPK signaling mediates resistance to PI3K inhibitors, these studies indicate that it is not necessarily the basal rate of MAPK activity that dictates resistance to PI3K pathway inhibitors, but the degree and kinetics of compensatory crosstalk. Thus while all four stable *PIK3CA* KD lines exhibited higher levels of pERK they were not more resistant to any of the PI3K pathway inhibitors than their CONSH counterparts. Similarly, increased activation of MAPK signaling did not alter the sensitivity of three of the four stable KD lines to MEK inhibition. Only the RMS-1 KD line, expressing 110β but not p110α or δ, exhibited increased sensitivity to the MEK inhibitor AZD6244. This suggests that p110β does not support compensatory activation of the PI3K pathway following MEK inhibition, whereas p110α and δ do.

Activated ERK signaling has been shown to activate mTOR by phosphorylation of both TSC2 and Raptor (32), and also to activate AMPK resulting in increased Rb phosphorylation and stimulation of cell growth (21). In addition, activated AMPK acts as a survival factor protecting cells from hypoxia and nutrient deprivation through increased

glucose uptake and a shift to anaerobic respiration with altered intermediary metabolism (the Warburg effect), often accompanied by inhibition of protein synthesis and cell growth through suppression of mTOR signalling (reviewed in (33)), Activation of AMPK along with deregulated IRS2 expression and an increased basal rate of autophagy (the latter prominent in the ERMS lines) suggests that mTOR signaling is partially compromised in the stable p110α KD lines. Importantly, these cells are more sensitive to TORC1/TORC2 inhibitors suggesting that mTOR is a central node for integrating crosstalk between the PI3K and MAPK pathways and an important target element for maximal PI3K pathway inhibition.

Dual blockade of both the PI3K and MAPK pathways was shown to be synergistic *in vitro* and was demonstrated to be due to the reciprocal inhibition of the compensatory activation of the alternate pathway seen following inhibition of each pathway individually. As predicted, treatment of the *NRAS* mutated RD tumor xenografts *in vivo* with the TORC1/TORC2 inhibitor AZD8055 or the MEK inhibitor AZD6244, showed no therapeutic benefit, while the dual PI3K/mTOR inhibitor NVP-BEZ235 was more active. However in combination, AZD8055/ AZD6244 resulted in significant inhibition of tumor growth while NVP-BEZ235/AZD6244 resulted in no additional benefit over treatment with NVP-BEZ235 alone. This was shown to be due to the inability of NVP-BEZ235 to inhibit the compensatory activation of AKT induced by MEK inhibition. Therefore, the biomarkers of effective activity are the simultaneous reduction of pAKT, pS6 and pERK.

Using data collected from Phase 1 clinical trials, a recent study has evaluated the clinical outcome of dual targeting both the PI3K and MAPK signaling pathways compared to targeting either pathway alone (34). The results showed increased efficacy in many tumor types but at the cost of additional toxicity. While the *in vivo* combination doses used here were well tolerated, PK analysis revealed an interaction between the two classes of compound resulting in lower plasma and tumor levels of AZD6244 but higher levels of the PI3K pathway inhibitors, both effects becoming more pronounced with repeat dosing. However, the concentrations of AZD6244 achieved *in vivo* were still in excess of levels required for MEK inhibition. Further PK/PD driven preclinical studies to identify the lowest AZD6244 dose required for MEK inhibition, followed by escalation of AZD8055 to achieve therapeutic efficacy will help inform early clinical trials. In addition, careful monitoring of plasma PKs of both drugs following repeat dosing will be required to assess the extent of drug-drug interactions in patients.

In summary, in the preclinical proof-of-principle RMS xenograft studies presented here, the combination of AZD8055 and AZD6244 showed significantly increased therapeutic benefit over the combination NVP-BEZ235/AZD6244. We show that the three phosphorylated biomarkers of ERK, S6 and AKT must be reduced for synergistic activity. These studies confirm that dual inhibition of both the PI3K and MAPK pathways offers a way forward for the treatment of those tumor types such as RMS that are predicted to be resistant to blockade of either pathway alone. Even in innately sensitive tumors, addition of a MEK inhibitor to a PI3K inhibitor may forestall the emergence of resistance.

Supplementary Material

Refer to Web version on PubMed Central for supplementary material.

Acknowledgments

The authors thank Chris Jones, Susanne Gatz, Paul Clark and Paul Workman for their review of the manuscript and helpful comments. We are grateful for help with tumor collection and annotation from the Children's Cancer and Leukemia Group.

Grant Support: This work was supported by NHS funding to the NIHR Biomedical Research Centre, the Royal Marsden Hospital Charitable funds, Cancer Research UK (grant references C309/A11566 and C5066/A10399), and the Chris Lucas Trust.

Funding: JR: NHS funding to the NIHR Biomedical Research Centre, KRT, RB: The Royal Marsden Hospital Charitable funds, MV, ADHB, SG, SAE, RRR, LDJ, FIR: Cancer Research UK (grant ref C309/A11566) JLS: the Chris Lucas Trust, ADP: CRUK and JS: CRUK (grant ref C5066/A10399).

References

1. De Giovanni C, Landuzzi L, Nicoletti G, Lollini PL, Nanni P. Molecular and cellular biology of rhabdomyosarcoma. Future Oncol. 2009; 5:1449–75. [PubMed: 19903072]
2. Xia SJ, Pressey JG, Barr FG. Molecular pathogenesis of rhabdomyosarcoma. Cancer Biol Ther. 2002; 1:97–104. [PubMed: 12170781]
3. Missiaglia E, Williamson D, Chisholm J, Wirapati P, Pierron G, Petel F, et al. PAX3/FOXO1 fusion gene status is the key prognostic molecular marker in rhabdomyosarcoma and significantly improves current risk stratification. J Clin Oncol. 2012; 30:1670–7. [PubMed: 22454413]
4. Martinelli S, McDowell HP, Vigne SD, Kokai G, Uccini S, Tartaglia M, et al. RAS signaling dysregulation in human embryonal Rhabdomyosarcoma. Genes Chromosomes Cancer. 2009; 48:975–82. [PubMed: 19681119]
5. Shukla N, Ameur N, Yilmaz I, Nafa K, Lau CY, Marchetti A, et al. Oncogene mutation profiling of pediatric solid tumors reveals significant subsets of embryonal rhabdomyosarcoma and neuroblastoma with mutated genes in growth signaling pathways. Clin Cancer Res. 2012; 18:748–57. [PubMed: 22142829]
6. Martins AS, Olmos D, Missiaglia E, Shipley J. Targeting the insulin-like growth factor pathway in rhabdomyosarcomas: rationale and future perspectives. Sarcoma. 2011; 2011:209736. [PubMed: 21437217]
7. Stevens MC. Treatment for childhood rhabdomyosarcoma: the cost of cure. Lancet Oncol. 2005; 6:77–84. [PubMed: 15683816]
8. Cen L, Hsieh FC, Lin HJ, Chen CS, Qualman SJ, Lin J. PDK-1/AKT pathway as a novel therapeutic target in rhabdomyosarcoma cells using OSU-03012 compound. Br J Cancer. 2007; 97:785–91. [PubMed: 17848913]
9. Petricoin EF 3rd, Espina V, Araujo RP, Midura B, Yeung C, Wan X, et al. Phosphoprotein pathway mapping: Akt/mammalian target of rapamycin activation is negatively associated with childhood rhabdomyosarcoma survival. Cancer Res. 2007; 67:3431–40. [PubMed: 17409454]
10. Engelman JA, Chen L, Tan X, Crosby K, Guimaraes AR, Upadhyay R, et al. Effective use of PI3K and MEK inhibitors to treat mutant Kras G12D and PIK3CA H1047R murine lung cancers. Nature Med. 2008; 14:1351–6. [PubMed: 19029981]
11. Weigelt B, Downward J. Genomic Determinants of PI3K Pathway Inhibitor Response in Cancer. Front Oncol. 2012; 2:109. [PubMed: 22970424]
12. Balmanno K, Chell SD, Gillings AS, Hayat S, Cook SJ. Intrinsic resistance to the MEK1/2 inhibitor AZD6244 (ARRY-142886) is associated with weak ERK1/2 signalling and/or strong PI3K signalling in colorectal cancer cell lines. Int J Cancer. 2009; 125:2332–41. [PubMed: 19637312]
13. Hoeflich KP, O'Brien C, Boyd Z, Cavet G, Guerrero S, Jung K, et al. In vivo antitumor activity of MEK and phosphatidylinositol 3-kinase inhibitors in basal-like breast cancer models. Clin Cancer Res. 2009; 15:4649–64. [PubMed: 19567590]
14. Wang Z, Zhou J, Fan J, Qiu SJ, Yu Y, Huang XW, et al. Effect of rapamycin alone and in combination with sorafenib in an orthotopic model of human hepatocellular carcinoma. Clin Cancer Res. 2008; 14:5124–30. [PubMed: 18698030]
15. Holt SV, Logie A, Davies BR, Alferez D, Runswick S, Fenton S, et al. Enhanced apoptosis and tumor growth suppression elicited by combination of MEK (selumetinib) and mTOR kinase inhibitors (AZD8055). Cancer Res. 2012; 72:1804–13. [PubMed: 22271687]

16. Tonelli R, McIntyre A, Camerin C, Walters ZS, Di Leo K, Selfe J, et al. Antitumor activity of sustained N-myc reduction in rhabdomyosarcomas and transcriptional block by antigene therapy. Clin Cancer Res. 2012; 18:796–807. [PubMed: 22065083]

17. Workman P, Aboagye EO, Balkwill F, Balmain A, Bruder G, Chaplin DJ, et al. Guidelines for the welfare and use of animals in cancer research. Br J Cancer. 2010; 102:1555–77. [PubMed: 20502460]

18. Raynaud FI, Eccles S, Clarke PA, Hayes A, Nutley B, Alix S, et al. Pharmacologic characterization of a potent inhibitor of class I phosphatidylinositide 3-kinases. Cancer Res. 2007; 67:5840–50. [PubMed: 17575152]

19. Chaussade C, Rewcastle GW, Kendall JD, Denny WA, Cho K, Gronning LM, et al. Evidence for functional redundancy of class IA PI3K isoforms in insulin signalling. Biochem J. 2007; 404:449–58. [PubMed: 17362206]

20. Harrington LS, Findlay GM, Gray A, Tolkacheva T, Wigfield S, Rebholz H, et al. The TSC1-2 tumor suppressor controls insulin-PI3K signaling via regulation of IRS proteins. J Cell Biol. 2004; 166:213–23. [PubMed: 15249583]

21. Rios M, Foretz M, Viollet B, Prieto A, Fraga M, Costoya JA, et al. AMPK Activation by Oncogenesis Is Required to Maintain Cancer Cell Proliferation in Astrocytic Tumors. Cancer Res. 2013; 73:2628–38. [PubMed: 23370326]

22. Foukas LC, Berenjeno IM, Gray A, Khwaja A, Vanhaesebroeck B. Activity of any class IA PI3K isoform can sustain cell proliferation and survival. Proc Natl Acad Sci USA. 2010; 107:11381–6. [PubMed: 20534549]

23. Serra V, Markman B, Scaltriti M, Eichhorn PJ, Valero V, Guzman M, et al. NVP-BEZ235, a dual PI3K/mTOR inhibitor, prevents PI3K signaling and inhibits the growth of cancer cells with activating PI3K mutations. Cancer Res. 2008; 68:8022–30. [PubMed: 18829560]

24. Kong D, Dan S, Yamazaki K, Yamori T. Inhibition profiles of phosphatidylinositol 3-kinase inhibitors against PI3K superfamily and human cancer cell line panel JFCR39. Eur J Cancer. 2010; 46:1111–21. [PubMed: 20129775]

25. Yeh TC, Marsh V, Bernat BA, Ballard J, Colwell H, Evans RJ, et al. Biological characterization of ARRY-142886 (AZD6244), a potent, highly selective mitogen-activated protein kinase kinase 1/2 inhibitor. Clin Cancer Res. 2007; 13:1576–83. [PubMed: 17332304]

26. Serra V, Scaltriti M, Prudkin L, Eichhorn PJ, Ibrahim YH, Chandarlapaty S, et al. PI3K inhibition results in enhanced HER signaling and acquired ERK dependency in HER2-overexpressing breast cancer. Oncogene. 2011; 30:2547–57. [PubMed: 21278786]

27. Sawyer C, Sturge J, Bennett DC, O'Hare MJ, Allen WE, Bain J, et al. Regulation of breast cancer cell chemotaxis by the phosphoinositide 3-kinase p110delta. Cancer Res. 2003; 63:1667–75. [PubMed: 12670921]

28. Boller D, Schramm A, Doepfner KT, Shalaby T, von Bueren AO, Eggert A, et al. Targeting the phosphoinositide 3-kinase isoform p110delta impairs growth and survival in neuroblastoma cells. Clin Cancer Res. 2008; 14:1172–81. [PubMed: 18281552]

29. Das F, Ghosh-Choudhury N, Dey N, Mandal CC, Mahimainathan L, Kasinath BS, et al. Unrestrained mammalian target of rapamycin complexes 1 and 2 increase expression of phosphatase and tensin homolog deleted on chromosome 10 to regulate phosphorylation of Akt kinase. J Biol Chem. 2012; 287:3808–22. [PubMed: 22184110]

30. Redondo-Munoz J, Escobar-Diaz E, Hernandez Del Cerro M, Pandiella A, Terol MJ, Garcia-Marco JA, et al. Induction of B-chronic lymphocytic leukemia cell apoptosis by arsenic trioxide involves suppression of the phosphoinositide 3-kinase/Akt survival pathway via c-jun-NH2 terminal kinase activation and PTEN upregulation. Clin Cancer Res. 2010; 16:4382–91. [PubMed: 20534739]

31. Kim S, Domon-Dell C, Kang J, Chung DH, Freund JN, Evers BM. Down-regulation of the tumor suppressor PTEN by the tumor necrosis factor-alpha/nuclear factor-kappaB (NF-kappaB)-inducing kinase/NF-kappaB pathway is linked to a default IkappaB-alpha autoregulatory loop. J Biol Chem. 2004; 279:4285–91. [PubMed: 14623898]

32. Carriere A, Cargnello M, Julien LA, Gao H, Bonneil E, Thibault P, et al. Oncogenic MAPK signaling stimulates mTORC1 activity by promoting RSK-mediated raptor phosphorylation. Curr Biol. 2008; 18:1269–77. [PubMed: 18722121]

33. Luo Z, Zang M, Guo W. AMPK as a metabolic tumor suppressor: control of metabolism and cell growth. Future Oncol. 2010; 6:457–70. [PubMed: 20222801]

34. Shimizu T, Tolcher AW, Papadopoulos KP, Beeram M, Rasco DW, Smith LS, et al. The clinical effect of the dual-targeting strategy involving PI3K/AKT/mTOR and RAS/MEK/ERK pathways in patients with advanced cancer. Clin Cancer Res. 2012; 18:2316–25. [PubMed: 22261800]

Europe PMC Funders Author Manuscripts

Europe PMC Funders Author Manuscripts

Translational Relevance

Molecular rationale to underpin the therapeutic use of PI3K/AKT/mTOR and RAS/RAF/MAPK pathway inhibitors is critical. Here we show co-activation of these pathways in 43% of primary rhabdomyosarcomas with most of the remainder exhibiting activation of the PI3K, but not MAPK, pathway. The former predicts resistance to single pathway-targeted agents and the latter, potential sensitivity to PI3K pathway inhibitors. However, we also demonstrate extensive compensatory signaling and cross-talk between the PI3K/MAPK pathways on inhibition of either pathway alone, both *in vitro* and *in vivo*. Therefore, simultaneous inhibition of both pathways is essential for effective treatment of rhabdomyosarcomas. The *in vivo* synergistic anti-tumor response achieved with the combination AZD8055/AZD6244 but not NVP-BEZ235/AZD6244, was reflected in reduction of the pharmacodynamic biomarkers pERK/pS6/p^{ser473}AKT. Preliminary pharmacokinetic analyses revealed drug-drug interactions between the PI3K/MAPK inhibitors studied indicating a requirement for pharmacokinetic analyses after repeat dosing in future clinical trials of the promising AZD8055/AZD6244 combination.

Europe PMC Funders Author Manuscripts

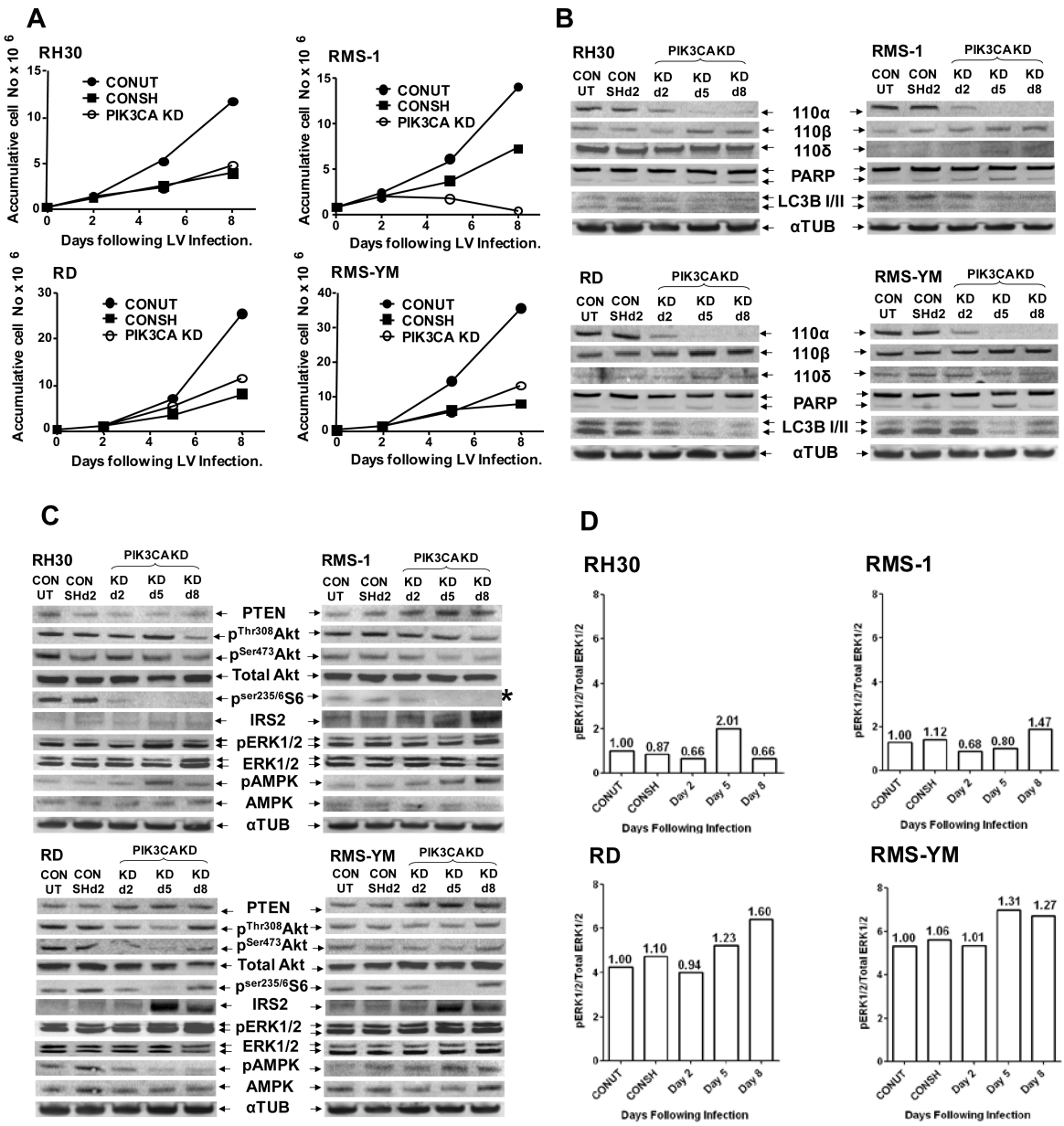

Figure 1. *PIK3CA* shRNA-mediated knockdown induces cell line-specific compensatory signaling and reciprocal cross-talk between the MAPK and PI3K pathways

A. Representative growth curves following *PIK3CA* knockdown: Two ARMS (RH30 and RMS-1) and two ERMS (RD and RMS-YM) cell lines were transduced with control (CONSH) or *PIK3CA* targeted shRNA (*PIK3CA* KD) on d0 or treated with polybrene only (CONUT). On d2, d5 and d8 cells were counted and on d2 and d5, an appropriate dilution was reseeded in fresh plates enabling accumulative cell counts to be calculated and plotted for d5 and d8. Puromycin (2.5μg/ml) selection was introduced on d2 and maintained for the entire experiment, the difference between the CONUT and CONSH growth curves being a reflection of viral transduction efficiency. **B.** Western immunoblots of Class 1A PI3K isoforms, confirming selective p110α KD over 8 days in the *PIK3CA* shRNA transduced cell lines, along with a marker for apoptosis (PARP cleavage) and autophagy (LCBI/II

expression). The PARP cleavage seen on d5 is a reflection of puromycin selection between d2-d5. **C.** Western immunoblots of PI3K pathway biomarkers showing cell line-specific disruption of PTEN, pAKT, pS6, IRS2, pERK and pAMPK in the above cells. * pS6 levels in RMS-1 cells were below the PhosphorImager detection levels. This image was therefore collected following 10mins exposure to X-ray film. **D.** Quantitation of pERK and total ERK immunoblots shown in **C.** using ImageQuant software, expressed as the ratio pERK:total ERK. Numbers above each bar: In each cell line the ratio of pERK:total ERK in the CONUT cells was set as 1.0 and the relative fold ratio change calculated for each sample.

Europe PMC Funders Author Manuscripts

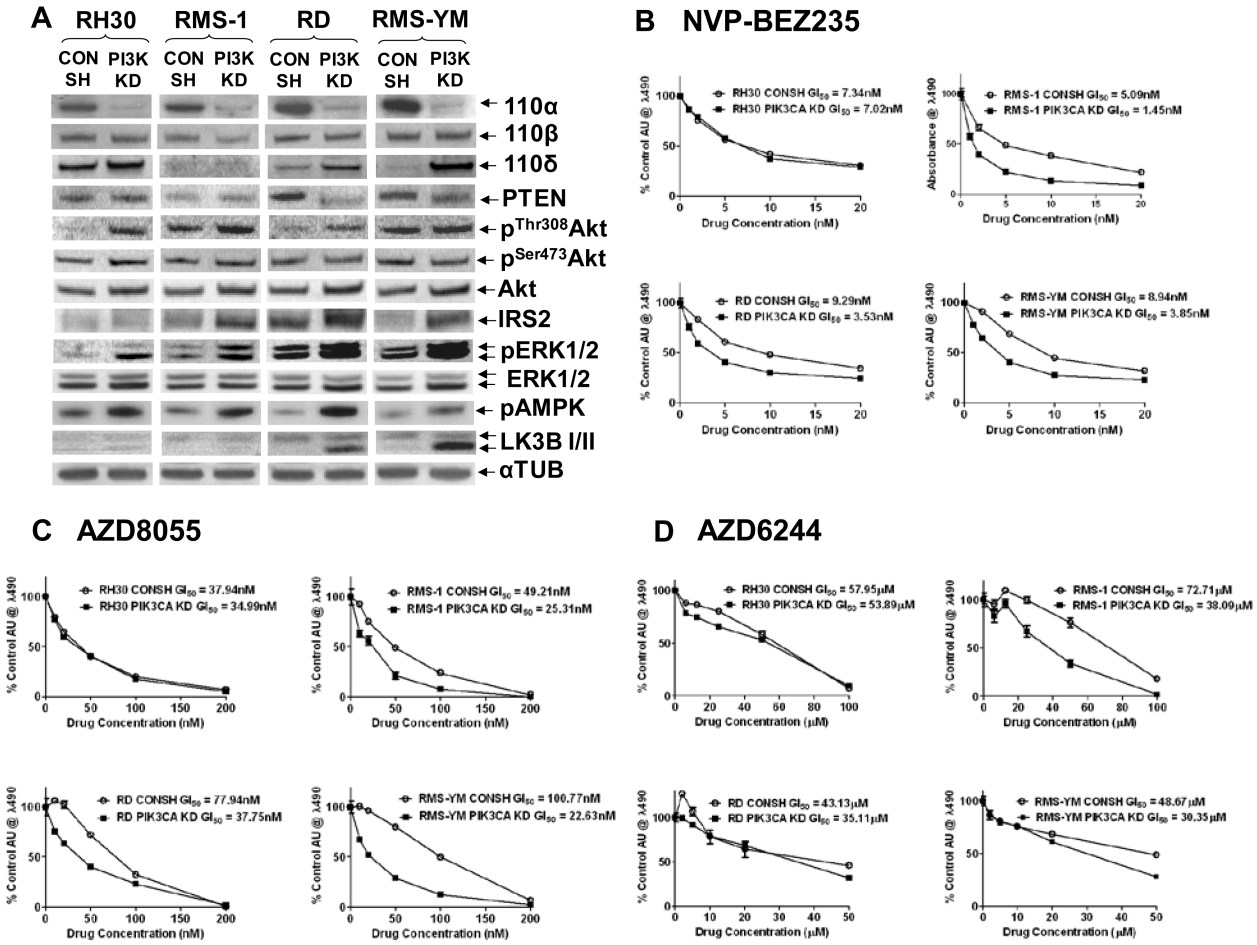

Figure 2. Reprogramming of the PI3K and MAPK signaling pathways induces increased sensitivity to mTOR inhibition in the stable p110α KD lines with deregulated IRS2 expression, but increased sensitivity to MEK inhibition only in RMS-1 KD cells with reduced p110α and δ expression

A. Western Immunoblots of Class 1A PI3K isoforms confirming p110α KD in the stable KD lines (PI3K KD) along with upregulation of p110δ expression in the ERMS KD stable lines compared to their CONSH counterparts. Also shown are selected elements of the PI3K and MAPK pathways in the stable p110α KD lines showing cell line-specific upregulation of p^{Thr308}AKT (but not p^{Ser473}AKT) and IRS2, upregulated pERK and pAMPK levels in all the KD lines, and increased autophagy (LCBI/II), particularly in the ERMS KD lines. **B.** and **C.** Representative growth inhibition curves, (MTS assays), following treatment of the paired CONSH and KD lines with NVP-BEZ235 and AZD8055 respectively, showing increased sensitivity to mTOR inhibition in the KD lines with deregulated IRS2 expression. **D.** Representative growth inhibition curves following treatment with the AZD6244 showing increased sensitivity to MEK inhibition only in RMS-1 cells lacking p110α and δ.

Europe PMC Funders Author Manuscripts

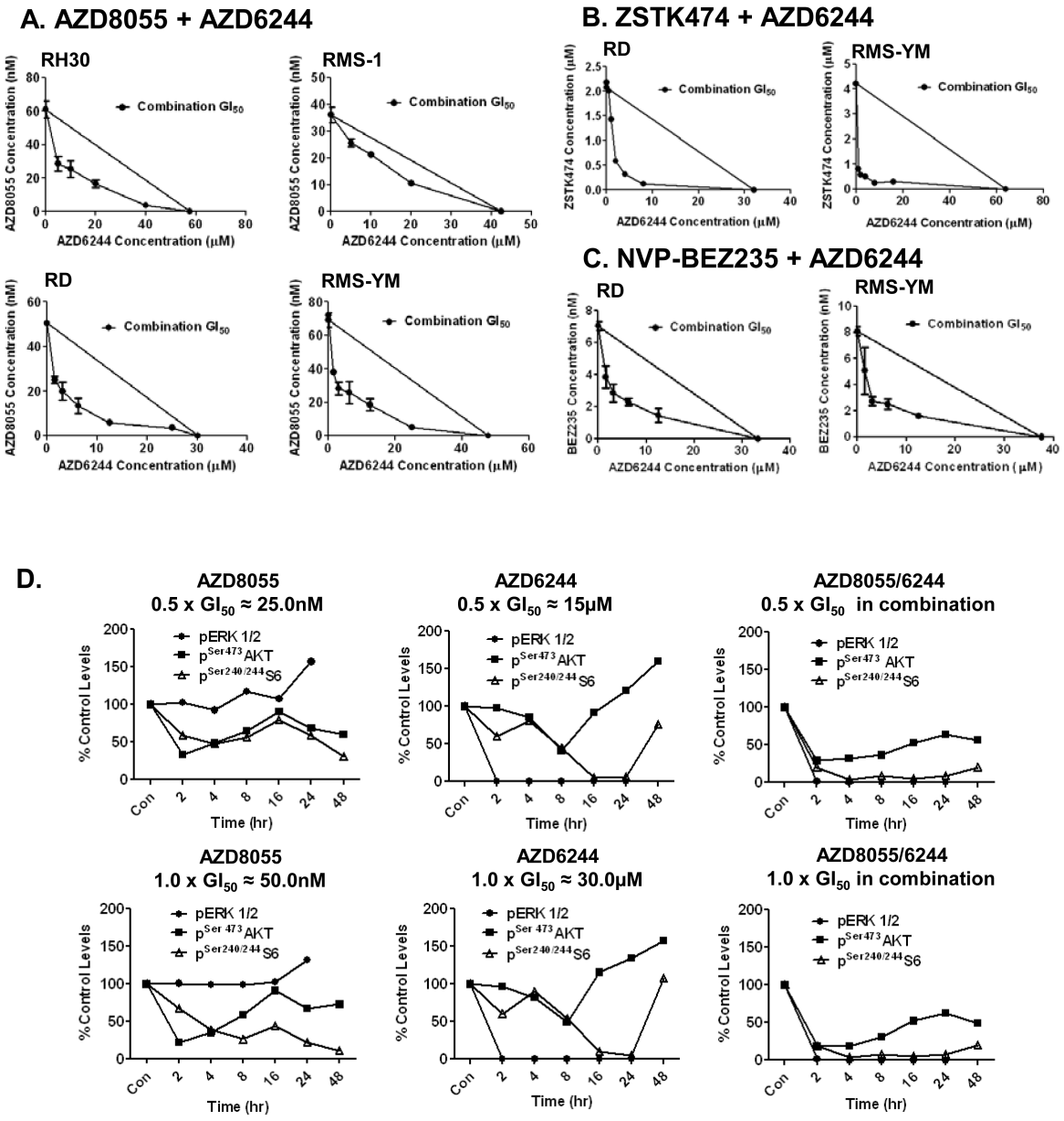

Figure 3. Dual blockade of both the PI3K and MAPK pathways is synergistic in RMS cell lines *in vitro*

A., B., and C. Combination isobolograms using the combinations: AZD8055/AZD6244, ZSTK474/AZD6244, and NVP-BEZ235/AZD6244 respectively. The GI_{50} values of compound A and B are plotted on the × and y axes along with the GI_{50} values of compound B obtained in the presence of various fixed concentrations of compound A. The diagonal line drawn between the GI_{50} values for the two compounds on the y and × axes is the theoretical line of additivity. All GI_{50} values to the left of this line indicate synergy. **D.** Levels of pERK1/2, p^{Ser473}AKT, and $p^{Ser240/244}$S6 in RD cells following treatment with AZD8055, AZD6244 and AZD8055/AZD6244 in combination at 0.5×, and 1.0× GI_{50} concentrations. Proteins from control and drug treated cells were extracted at the indicated time points following treatment. Control and treated samples from each time point were

Europe PMC Funders Author Manuscripts

loaded side by side for western immunoblots and quantitated using ImageQuant software. Drug treated/control phosphorylated biomarker levels at each time point are expressed as % of levels at time 0. NB. Levels of pERK in control samples were below consistently quantifiable levels at 48h, when the cells were reaching confluence.

Europe PMC Funders Author Manuscripts

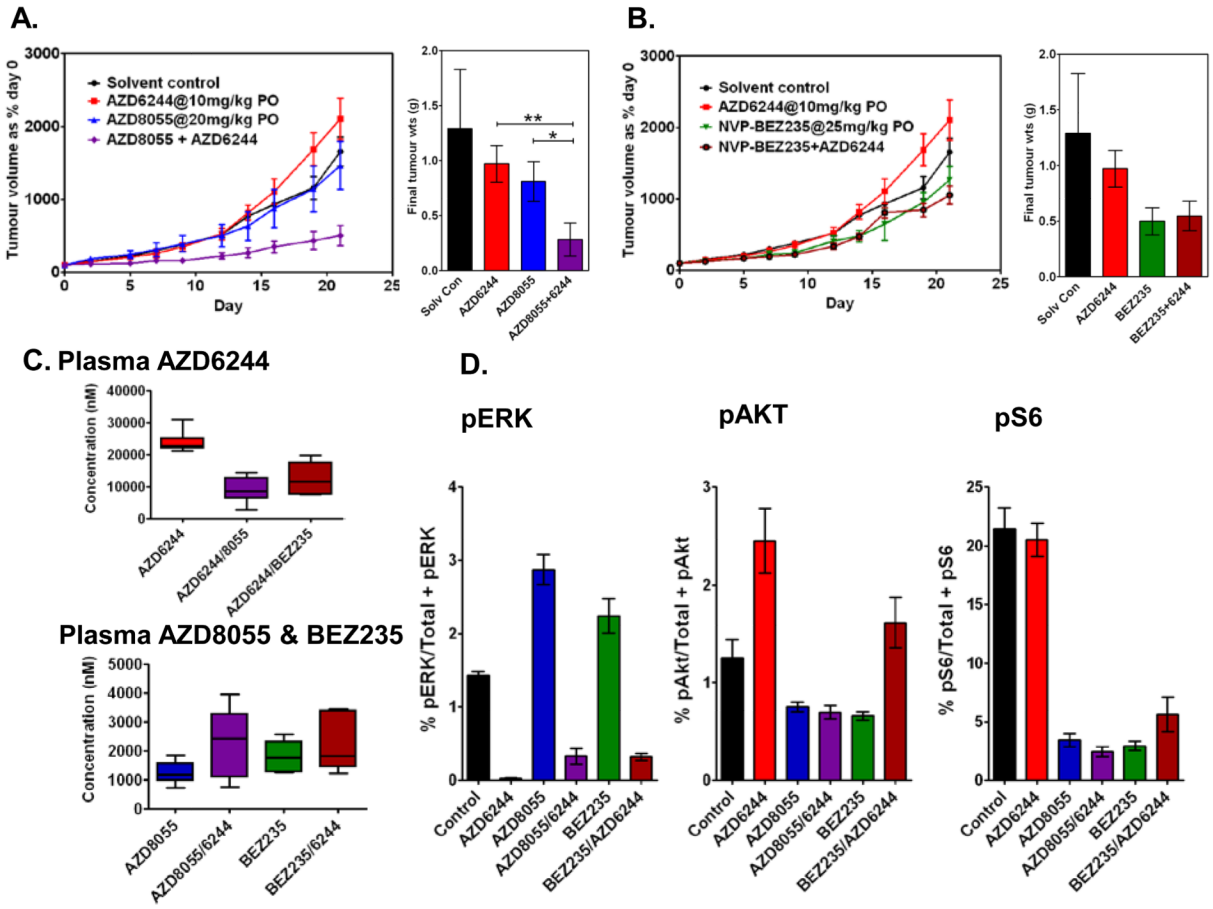

Figure 4. Significantly enhanced antitumor efficacy following treatment of RD xenografts with AZD8055, but not NVP-BEZ235, in combination with AZD6244

A. and **B.** Head-to-head therapeutic study of RD xenografts treated with AZD6244 and either AZD8055 or NVP-BEZ235 respectively at the indicated doses alone, and in combination. Tumor volumes are expressed as a % volume of each tumor on day 0. Final tumor weights (g) show significantly increased efficacy of the combination AZD8055/ AZD6244 compared with AZD6244 alone (**p=0.015) or AZD8055 alone (*p=0.038) and no significant difference in efficacy of the combination NVP-BEZ235/ AZD6244 compared with AZD6244 alone (p=0.13) or BEZ235 alone (p=0.82) (Mann Whitney t test). **C.** Plasma AZD6244 concentrations 3hrs following the final dose in mice treated with AZD6244 alone or in combination with AZD8055 or NVP-BEZ235 and plasma AZD8055 and NVP-BEZ235 concentrations from the same mice as above. **D.** Tumor PD biomarkers pERK: phospho(T/Y:202/204:185/187)ERK/total ERK1/2, pAKT: phospho(Ser473)AKT/total AKT and pS6: phospho(240/244)S6/total S6, as determined by MSD immunoassay.

Europe PMC Funders Author Manuscripts